



Scholars' Mine

Masters Theses

Student Theses and Dissertations

1970

Digital simulation of a Costas loop demodulator in Gaussian noise and CW interference

Ajay Mugatlal Mehta

Follow this and additional works at: https://scholarsmine.mst.edu/masters_theses

 Part of the [Electrical and Computer Engineering Commons](#)

Department:

Recommended Citation

Mehta, Ajay Mugatlal, "Digital simulation of a Costas loop demodulator in Gaussian noise and CW interference" (1970). *Masters Theses*. 7048.

https://scholarsmine.mst.edu/masters_theses/7048

This thesis is brought to you by Scholars' Mine, a service of the Missouri S&T Library and Learning Resources. This work is protected by U. S. Copyright Law. Unauthorized use including reproduction for redistribution requires the permission of the copyright holder. For more information, please contact scholarsmine@mst.edu.

DIGITAL SIMULATION OF A COSTAS LOOP DEMODULATOR
IN GAUSSIAN NOISE AND CW INTERFERENCE

By

AJAY MUGATLAL MEHTA, 1947 -

A

THESIS

submitted to the faculty of

THE UNIVERSITY OF MISSOURI - ROLLA

in partial fulfillment of the requirements for the

Degree of

MASTER OF SCIENCE IN ELECTRICAL ENGINEERING

Rolla, Missouri

1970

Approved by

R. E. Ziemer (Advisor)

William H. Tamm

Thomas Baird

ABSTRACT

A digital computer model of a Costas loop has been employed to study the effects of Gaussian noise and continuous-wave interference on the detection of biphase modulated signals. The dependence of bit-error probability, mean-square error between input and output, phase-error variance and threshold on signal-to-Gaussian-noise power ratio, interference-to-Gaussian-noise power ratio and frequency offset of the interference have been investigated and compared with previously obtained experimental results. The model has been verified for its accuracy in the case of no noise and when Gaussian noise is present at its input.

TABLE OF CONTENTS

	Page
ABSTRACT	ii
LIST OF FIGURES	iv
LIST OF TABLES	v
ACKNOWLEDGEMENTS	vi
I. INTRODUCTION	1
II. DERIVATION OF THE COMPUTER MODEL	3
A. EQUATIONS FOR COSTAS LOOP OPERATION IN NOISE AND INTERFERENCE	3
B. IMPLEMENTATION OF THE LOOP EQUATIONS AS A COMPUTER MODEL	11
III. VERIFICATION OF THE MODEL AND RESULTS.	17
A. VERIFICATION OF MODEL.	17
B. RESULTS FOR INTERFERENCE BACK- GROUNDS	29
IV. DISCUSSION OF RESULTS AND CONCLUSIONS.	32
REFERENCES	35
VITA	37
APPENDICES	
A. FLOW DIAGRAM - NOISELESS CASE	38
B. COMPUTER PROGRAM - NOISELESS CASE	40
C. FLOW DIAGRAM - GAUSSIAN NOISE AND CW INTERFERENCE PRESENT	44
D. COMPUTER PROGRAM - GAUSSIAN NOISE AND CW INTERFERENCE PRESENT	48

LIST OF FIGURES

Figure		Page
1.	Block Diagram of a Costas Loop Demodulator	4
2.	Power Spectral Density of the Gaussian Sampling Processes	14
3.	Transient Response of the Model - Noiseless Case 1	20
4.	Transient Response of the Model - Noiseless Case 2	22
5.	Example of the Effect of Seed Selection . .	24
6.	Flow Diagram for Computer Model - Noiseless Case 2	39
7.	Flow Diagram for Computer Model - Gaussian Noise and cw Interference Present	45

LIST OF TABLES

Table		Page
1	Bit-Error Probability vs SNRDB	26
2	Phase-Error Variance vs SNRDB.	26
3	Threshold Results for Costas Loop	28
4	Summary of Results for MSE in Presence of cw Interference	30
5	Summary of Results for P_E in Presence of cw Interference	31

ACKNOWLEDGEMENTS

The author wishes to express his sincere gratitude to Dr. R.E. Ziemer for his very valuable guidance and help during the course of this study. Thanks are also due to Dr. William H. Tranter for his very useful comments in the writing of this thesis.

The author is also thankful to all others who contributed towards the completion of this thesis.

I. INTRODUCTION

A numerical technique for conducting statistical sampling experiments on a model of a system to obtain a probabilistic approximation to the behavior of the system is called Monte Carlo simulation. The model of the system must be describable in a logical and/or mathematical manner. In general, the simulation is carried on a digital computer, not because of any basic relationship, but because of the very large amount of calculations required.

This thesis is concerned with the development of a digital computer model of a Costas loop demodulator and simulating the effects of Gaussian noise and continuous-wave (cw) interference on the demodulation of phase shift keyed (PSK) signals. Interference is commonly encountered in many applications of Costas loops, e.g., in telemetry systems where the interference is due to extraneous sources. The simulation technique consists of integrating the loop equations by using the Runge-Kutta method of order IV [1].

Costas loops are similar to phase-lock loops (PLLs) in that both can be used to demodulate signals which are digitally phase modulated. The difference, however, is that a PLL requires carrier component to lock onto, but a

Costas loop does not. A more complete description of the operation of a Costas loop will be given later. Because of the intractable mathematical nature of the problem, computer modeling appears to be one of few ways available for obtaining useful results.

Digital computer simulation of PLL's in Gaussian noise has been carried out before [2,3]. Simulation of PLL operation in multipath backgrounds has also been done previously [4], and theoretical analyses of Costas loops operating in Gaussian noise are also obtainable in the literature [5]. However, few results are available on the effects of interference on such devices.

The performance of the Costas loop considered in this thesis is characterized in terms of (1) bit-error probability, (2) normalized mean-square error between input and output, (3) threshold, and (4) phase-error variance. Results are obtained for different values of (i) signal-to-Gaussian-noise power ratio, (ii) interference-to-Gaussian-noise power ratio, and (iii) frequency offset of interference. Previously obtained experimental results [6] will be used to compare with and verify the accuracy of the simulation.

II. DERIVATION OF THE COMPUTER MODEL

A. Equations for Costas Loop Operation in Noise and Interference

In this chapter the equations describing the operation of the Costas loop are derived. These equations will then be used to develop the computer model. Figure 1 shows a block diagram representation of a Costas loop demodulator. The equations which describe the operation of the loop with signal, Gaussian noise, and cw interference at its input will now be obtained. The digital computer model consists of a numerical solution of these equations, as will be described later.

Let $y(t)$ be the input to the Costas loop. It consists of the suppressed carrier signal, $s(t)$, plus Gaussian noise, $n_g(t)$, plus cw interference, $n_i(t)$. Thus, $y(t)$ can be written as

$$y(t) = s(t) + n_g(t) + n_i(t) \quad (2-1)$$

The signal $s(t)$ is represented as

$$s(t) = \sqrt{2} A m(t) \sin(\omega_0 t + \theta), \quad (2-2)$$

where

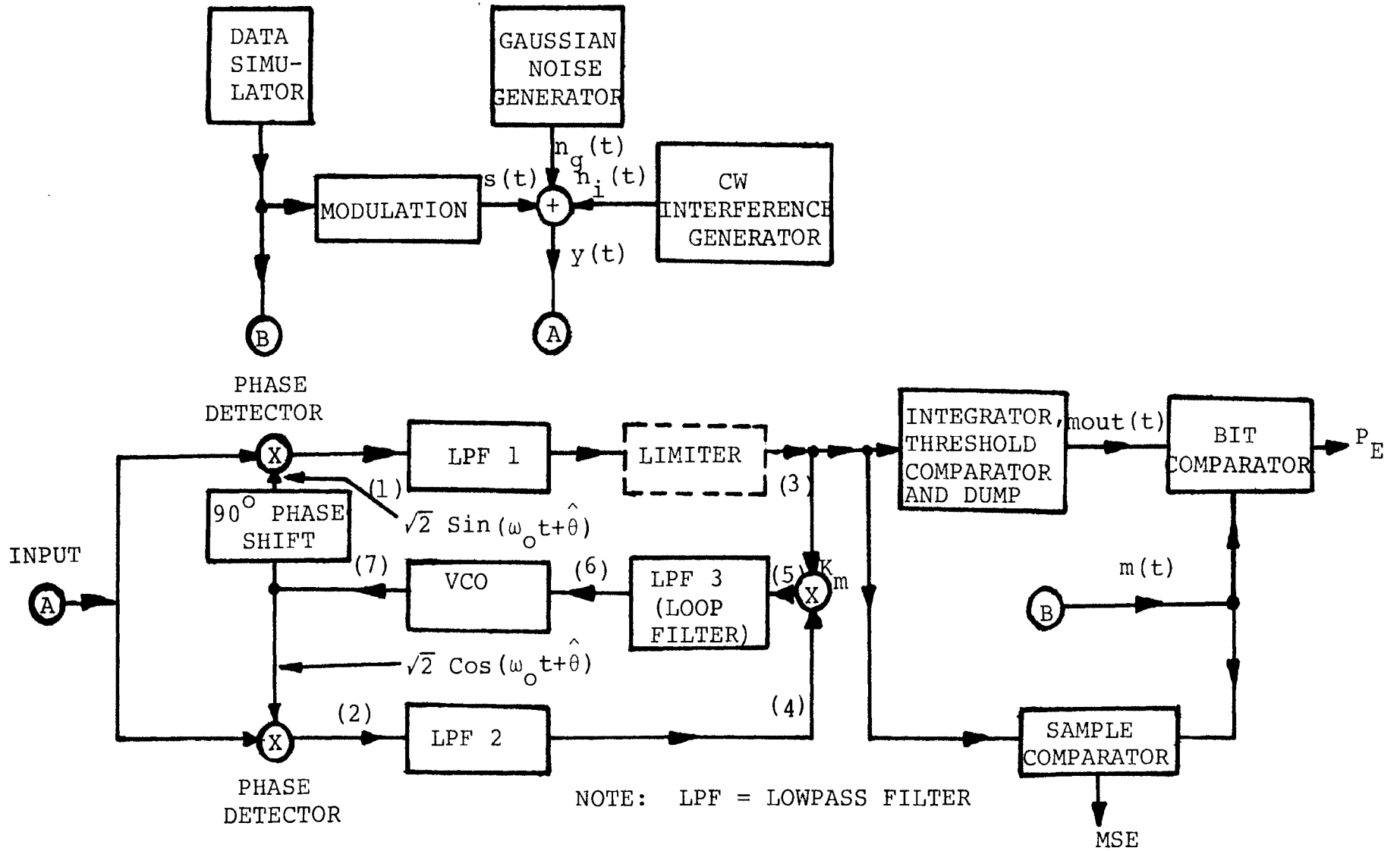


Figure 1. Block Diagram of a Costas Loop Demodulator

A = constant amplitude factor,

$m(t)$ = modulation or signal envelope,

ω_o = frequency of the carrier in radians/second,

and

θ = random phase angle of the carrier,

Assuming that the noise $n_g(t)$ is narrow-band, zero-mean, and Gaussian, it can be represented as [7]

$$n_g(t) = \sqrt{2} n_1(t) \cos(\omega_o t + \theta) + \sqrt{2} n_2(t) \sin(\omega_o t + \theta) \quad (2-3)$$

where $n_1(t)$ and $n_2(t)$ are statistically independent sample functions of a jointly stationary Gaussian process. The power spectral densities of $n_1(t)$ and $n_2(t)$ are N_o watts/Hz, single-sided, over the passband 0 to $W/2$ Hz and zero elsewhere, if that of $n_g(t)$ is N_o watts/Hz, single-sided, over the passband $f_o - W/2$ to $f_o + W/2$ Hz ($f_o = \omega_o / 2\pi$) and zero elsewhere. Thus,

$$\overline{n_g^2(t)} = 2\overline{n_1^2(t)} = 2\overline{n_2^2(t)} = N_o W \quad (2-4)$$

The cw interference can be represented as

$$\begin{aligned} n_i(t) &= \sqrt{2} b_o \sin[(\omega_o + \Delta\omega)t + \theta + \delta] \\ &= \sqrt{2} b_o \sin(\Delta\omega t + \delta) \cos(\omega_o t + \theta) \\ &\quad + \sqrt{2} b_o \cos(\Delta\omega t + \delta) \sin(\omega_o t + \theta), \quad (2-5) \end{aligned}$$

where the randomly varying phase difference between the signal and the interference is represented as δ .

Equation (2-5) can be written in the same form as Eq. (2-3), so that

$$n_i(t) = \sqrt{2} n_{ic} \cos(\omega_o t + \theta) + \sqrt{2} n_{is} \sin(\omega_o t + \theta) \quad (2-6)$$

where

$$n_{ic} = b_o \sin(\Delta\omega t + \delta) \quad (2-7a)$$

and

$$n_{is} = b_o \cos(\Delta\omega t + \delta) \quad (2-7b)$$

The lowpass filters LPF 1 and LPF 2 are assumed to have the following effects on the signal, noise, and interference components at points (1) and (2) in Figure 1:

- (1) The low frequency components of signal are passed without distortion;
- (2) The low frequency components of the noise are passed without distortion;
- (3) All double frequency components are completely rejected;
- (4) The only effect on the cw interference is attenuation and phase shift of its low frequency components in accordance with the filter transfer function, which is represented as

$$H(\omega) = B(\omega) \exp[j\theta(\omega)], \quad (2-8)$$

where

$B(\omega)$ = amplitude response function of the lowpass filters

and

$\theta(\omega)$ = phase shift function of the lowpass filters.

Let the output of the VCO (point (7) in Figure 1) be

$$V_7(t) = \sqrt{2} \cos(\omega_0 t + \hat{\theta}) \quad (2-9)$$

where $\omega_0/2\pi$ is the free-running frequency of the VCO in Hz, and $\hat{\theta}$ is the Costas loop's estimate of the unknown phase θ . The output $V_3(t)$ of LPF 1 is the same as the low frequency components of the output $V_1(t)$ of the upper phase detector except that the low frequency components of interference will be attenuated and phase shifted according to the transfer function $H(\omega)$ as defined by Eq. (2-8). Thus,

$$\begin{aligned} V_3(t) = & A_m(t) \cos\vartheta - n_1(t) \sin\vartheta + n_2(t) \cos\vartheta \\ & - b_0 B(\Delta\omega) \sin[\Delta\omega t + \delta + \theta(\Delta\omega)] \sin\vartheta \\ & + b_0 B(\Delta\omega) \cos[\Delta\omega t + \delta + \theta(\Delta\omega)] \cos\vartheta \end{aligned} \quad (2-10)$$

where

$$\vartheta = \theta - \hat{\theta} \quad (2-11)$$

is the phase-error.

Similarly, the output of LPF 2 can be written as

$$\begin{aligned}
 V_4(t) = & A m(t) \sin \theta + n_1(t) \cos \theta + n_2(t) \sin \theta \\
 & + b_o B(\Delta \omega) \sin [\Delta \omega t + \delta + \theta(\Delta \omega)] \cos \theta \\
 & + b_o B(\Delta \omega) \cos [\Delta \omega t + \delta + \theta(\Delta \omega)] \sin \theta
 \end{aligned} \tag{2-12}$$

The differential equation describing the loop is

$$\frac{d\hat{\theta}(t)}{dt} = K_v F(p) V_5(t) \tag{2-13}$$

where

$p = d/dt$ is the differential operator,

K_v = multiplying constant for the VCO,

$F(p)$ = transfer function of the loop filter LPF 3,

and

$V_5(t)$ = voltage at point (5) in Figure 1.

From Figure 1,

$$V_5(t) = K_m V_3(t) V_4(t), \tag{2-14}$$

where K_m is the multiplier constant.

In practice, the characteristics of a second order loop are conveniently specified in terms of its damping factor ζ and the natural frequency of oscillation ω_n , or the equivalent noise bandwidth, W_L , of the linearized loop.

These parameters can be defined in terms of various loop and signal constants. From Eqs. (2-10) and (2-14), the differential equation for the linearized loop with only signal present at the input is

$$\frac{d\hat{\theta}}{dt} = K_v K_m A^2 F(p) (\theta - \hat{\theta}) \quad (2-15)$$

where the approximation $\sin 2\theta \approx 2\theta$ has been used. The closed loop transfer function $H_o(s)$ can be defined as the ratio of the Laplace transform of $\theta(t)$ to that of $\hat{\theta}(t)$, and from Eq. (2-15), is

$$H_o(s) = \frac{Y(s)}{1+Y(s)}, \quad (2-16)$$

where

$$Y(s) = K_v K_m A^2 F(s)/s \quad (2-17)$$

is referred to as the open loop transfer function.

Equation (2-17) is written under the assumption that $m(t) = \pm 1$, i.e., $m(t)$ is a binary digital sequence.

Assuming $F(s)$ to be the filter transfer function of a perfect second-order active loop, i.e.,

$$F(s) = 1 + \frac{a}{s}, \quad (2-18)$$

it can be easily shown that

$$H_o(s) = \frac{2\zeta\omega_n s + \omega_n^2}{s^2 + 2\zeta\omega_n s + \omega_n^2} \quad (2-19)$$

where

$$a = \omega_n / 2\zeta, \quad (2-20)$$

and

$$2\zeta\omega_n = A^2 K_v K_m. \quad (2-21)$$

A commonly used value for the damping factor in PLL work is $\zeta = 0.707$ [8]. This value for ζ will be used here. The natural frequency ω_n is conveniently specified in terms of ζ and the equivalent noise bandwidth W_L of the loop, by

$$\omega_n = \frac{4\zeta W_L}{1+4\zeta^2} \quad (2-22)$$

The parameter W_L is defined by

$$W_L = 2B_L = \int_{-\infty}^{\infty} \left| \frac{Y(f)}{1+Y(f)} \right|^2 df \quad (2-23)$$

where $Y(f)$ is given by Eq. (2-17) with $s = j2\pi f$.

Even for the nonlinear case, it is usually most convenient to describe the second-order loop in terms of ζ and ω_n (or W_L) which are parameters that have been defined for the linearized loop. When Eq. (2-13) is expressed in terms of ζ and ω_n , for a loop filter with transfer function given by Eq. (2-18), it becomes

$$\frac{d^2 \hat{\theta}}{dt^2} = 2\zeta\omega_n \frac{d}{dt} \left(\frac{V_5}{K_m} \right) + \omega_n^2 \left(\frac{V_5}{K_m} \right) \quad (2-24)$$

This last equation along with Equations (2-10), (2-12), (2-14) and (2-22) completely describes the loop action in terms of the desired parameters W_L and ζ in response to the signal, noise and interference.

For the purpose of numerical integration, Eq. (2-24) can be represented as two simultaneous differential equations of first order [1]. If $\hat{\theta} = y$, and z is introduced as a dummy variable, Eq. (2-24) is equivalent to

$$\frac{dy}{dt} = z + 2\zeta \omega_n \left(\frac{V_5}{K_m}\right) \quad (2-25)$$

and

$$\frac{dz}{dt} = -\omega_n^2 \left(\frac{V_5}{K_m}\right) \quad (2-26)$$

These are the equations which are numerically integrated in the digital computer model of the loop. This model will be described in the next section.

B. Implementation of the Loop Equations as a Computer Model

The equations derived in the previous section that describe the Costas loop operation are first represented as a flow diagram to facilitate the development of the computer program for the model. Two such flow diagrams are shown in Appendices A and C. The first one is for the noiseless case and is a much simplified version of

the second one, which includes Gaussian noise and cw interference. The flow diagrams are presented in the logical form and show the major steps implemented in the computer program (Appendices B and D) written for the model.

From the flow diagram for the model with interference it will be noted that a limiter is included in the in-phase channel of the loop. This was done mainly to simulate the actual loop used to obtain the experimental results which included a limiter. It stabilizes the loop response at high noise and interference levels.

The results presented in the next section were obtained only for a few specific cases, because (i) only a limited number of experimental results [6] were available for comparison and verification of the model and (ii) availability of computer time was limited. However, the flow diagram presented in Appendix C is quite general and is flexible enough to allow a selection of loop characteristics such as amplitude response function $B(\omega)$ of the in-phase and quadrature-phase channel filters (LPF1 and LPF2) to the low frequency components of interference, the loop bandwidth W_L , and the damping factor ζ . Two types of modulating signals can be selected, namely, a random binary sequence or periodic binary sequences such as a pseudo-random maximal-length

sequence [9]. In practice, purely random sequences with known properties are difficult to generate and use. Therefore, periodic pseudo-random sequences of finite length are often employed to simulate digital data.

A normal random number generator (available in the Scientific Subroutine Package (SSP) memory of the computer) was employed to generate noise samples for the two Gaussian processes $n_1(t)$ and $n_2(t)$ (refer to Figure 7). The standard deviation for these Gaussian samples was calculated as follows.

Assume a sample is taken every

$$T_I = \frac{T_b}{\text{SPB}} \text{ seconds,} \quad (2-27)$$

where

T_b = period of a data bit,

and

SPB = number of samples per bit

Also, let the variance of each noise sample be σ^2 . We want σ^2 in terms of the signal-to-Gaussian-noise ratio (SNR) and SPB. Let the noise bandwidth be B Hz and the noise power spectral density be N_0 watts/Hz, as shown in Figure 2.

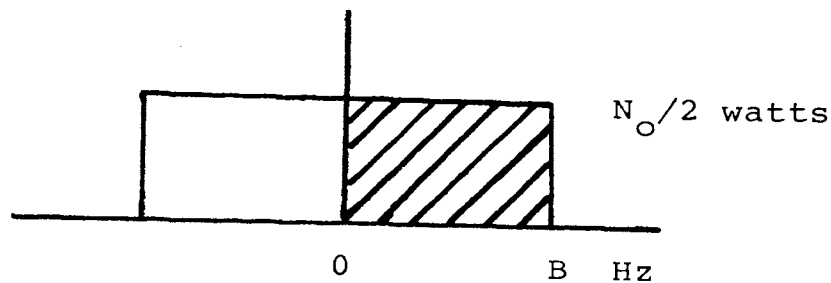


Figure 2: Power Spectral Density of the Gaussian Sampling Processes

Thus,

$$\sigma^2 = N_o B \quad (2-28)$$

and, for the samples to be independent, we must sample at the Nyquist rate [10], or

$$T_I = \frac{1}{2B} \quad (2-29)$$

Substituting for B in Equation (2-28) from Equation (2-29) we obtain

$$\sigma^2 = \frac{N_o}{2T_I} \quad (2-30)$$

The signal-to-Gaussian noise ratio is defined

as

$$\text{SNR} = \frac{A^2 T_b}{N_o} \quad (2-31)$$

where the noise power is measured in a bit-rate bandwidth $f_b = 1/T_b$. From Equations (2-27), (2-30) and (2-31) we obtain

$$\sigma^2 = \frac{\text{SPB}}{2 \times \text{SNR}} \quad (2-32a)$$

where $A = 1$ for convenience (i.e., all power levels are normalized to the power in the signal). Thus, the standard deviation σ of each noise sample is

$$\sigma = \left(\frac{\text{SPB}}{2 \times \text{SNR}} \right)^{1/2}. \quad (2-32b)$$

The filters LPF 1 and LPF 2 were assumed to be a cascade of two one-pole lowpass stages, having an amplitude response function

$$B(f) = \frac{1}{1 + (f/\alpha)^2} \quad (2-33)$$

where α is the cut-off frequency of the filter.

From Equation (2-5), the interference power is b_0^2 . However, the signal power has been assumed to be unity (for convenience), so the amplitude b_0 of the cw interference can be calculated for the model as

$$\begin{aligned} b_0^2 &= \text{Interference Power} \\ &= \frac{\text{Interference Power}}{\text{Signal Power}} = \frac{\text{INR}}{\text{SNR}} \end{aligned} \quad (2-34a)$$

or

$$b_0 = \left(\frac{\text{INR}}{\text{SNR}} \right)^{1/2}. \quad (2-34b)$$

The relations derived in this section were employed to calculate different parameters for the computer model from the given values of the standard parameters ζ , W_L , INR, SNR, Δf , f_b , etc. for the Costas loop.

III. VERIFICATION OF THE MODEL AND RESULTS

Once the computer model was obtained, its validity and accuracy were tested by comparing simulation results with known theoretical results for loop operation under various conditions but without cw interference. The effects of cw interference on Costas loop operation were then studied for a few specific cases by using the model.

A. Verification of Model

The major steps taken in verifying the accuracy of the digital computer model of a Costas loop operating in interference were the following:

1. Selection of a proper method for solving the differential equation of the Costas loop

Before adopting the Runge-Kutta method of order IV for the differential equation of the loop, the RKGS and HPCG subroutines available in the SSP memory of the computer were first used. Neither of these methods were suitable, as in trying to satisfy a specified error, they have the inherent tendency to reduce the step size. This in turn, made it impossible to calculate the standard deviation of the Gaussian-noise samples used to simulate

$n_1(t)$ and $n_2(t)$ from the known signal-to-Gaussian-noise ratio, because of the resulting unknown number of samples used per bit. The Runge-Kutta method of order IV for solving two simultaneous differential equations of first order [1] with a fixed size integration (i.e. sampling) interval, h , was then used and found acceptable.

2. Testing the model for transient response under noiseless conditions

Testing of the model for transient response was accomplished for two inputs, namely, signal with initial frequency offset from the VCO frequency, and an input signal with increasing frequency offset.

Case 1: Constant Frequency Offset

For the constant frequency offset case, the input signal is

$$s(t) = \sqrt{2} A_m(t) \cos(\omega_o t + \theta) \quad (3-1)$$

where

$$\theta = \Omega t u(t) \quad (3-2)$$

That is, the initial frequency offset of the signal is Ω radians/second from the initial frequency of the VCO.

With small phase error and for no noise and interference, Eqs.(2-10), (2-12) and (2-14) simplify to

$$\frac{V_5(t)}{K_m} = \frac{1}{2} \sin 2\theta \approx \theta, \quad (3-3)$$

when $A = 1$ (assumed for convenience).

Substituting into Eq. (2-24) and solving for the phase error θ we get, for $\zeta = 0.707$,

$$\theta(t) = \sqrt{2} \frac{\Omega}{\omega_n} \exp\left(-\frac{\omega_n}{\sqrt{2}}t\right) \sin\left(\frac{\omega_n}{\sqrt{2}}t\right) u(t). \quad (3-4)$$

Linear operation of the loop imposes the condition that $|\theta_{\max}| \ll 1$ radian. It can be shown that in terms of Ω this requires

$$\Omega \ll 3.2W_L \quad (3-5)$$

for the damping factor used.

A plot of phase error, θ , versus time, as obtained from Eq. (3-4), is shown in Figure 3. The phase error obtained from the computer model is also shown. For $\Omega=10$ and $W_L=100$, the condition of linearity is satisfied and the two plots coincide exactly. This indicates that the basic computer model is accurate for noiseless inputs. Also shown in Figure 3 is the response of the model for $\Omega=200$, which shows the deviation from linearity when a value of Ω is used that does not satisfy the inequality in Eq. (3-5).

Case 2. Linearly increasing frequency

The phase of the carrier for a linearly increasing frequency is

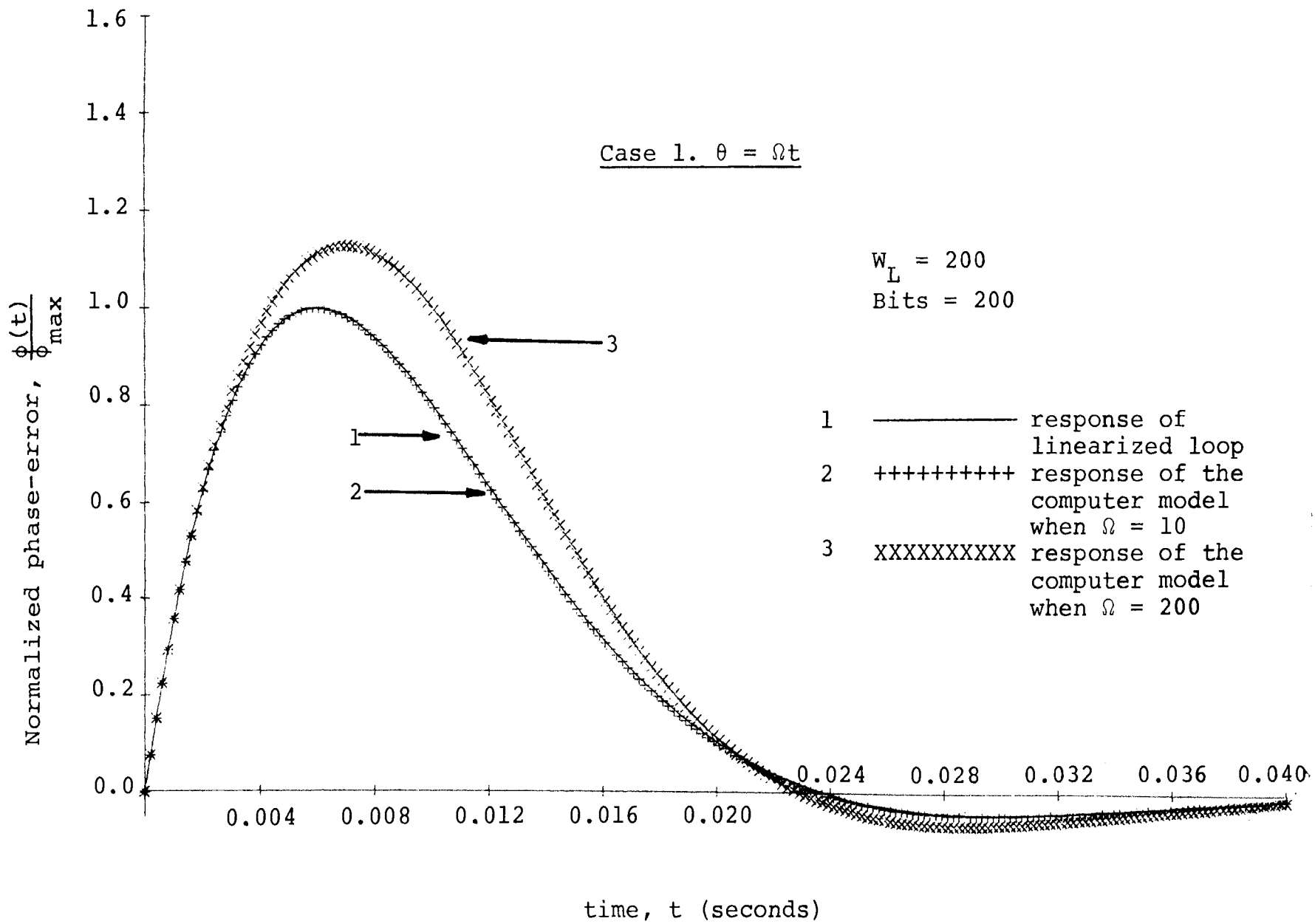


Figure 3. Transient Response of the Model - Noiseless Case 1.

$$\theta = \frac{1}{2}Dt^2 u(t). \quad (3-6)$$

The solution of the linearized differential equation of the loop for this input phase is

$$\vartheta(t) = \frac{D}{\omega_n} [1 - \sqrt{2} \exp(-\frac{\omega_n t}{\sqrt{2}}) \cos(\frac{\omega_n}{\sqrt{2}} t - \frac{\pi}{4})] \quad (3-7)$$

and the condition of linearity, $|\vartheta_{\max}| \ll 1$, leads to

$$D \ll 8/9 W_L^2 \quad (3-8)$$

for $\zeta = 0.707$.

A comparison of $\vartheta(t)$ calculated from the linearized differential equation with $\vartheta(t)$ obtained from the computer model is given in Fig. 4 for two values of D . For $D=10$, the condition for linearity, Eq. (3-8), is satisfied, while for $D=10000$, the model is operating in the non-linear region. Again, as in the previous case, the plot obtained from the linearized solution coincides exactly with the response of the model as long as condition for linearity is satisfied. This further verifies the accuracy of the model under noiseless conditions.

3. Selection of proper seeds for the random Gaussian number generators

Seed for a random number generator is a number to be specified and used as a starting point in generating the random number sequence. Proper selection of seeds

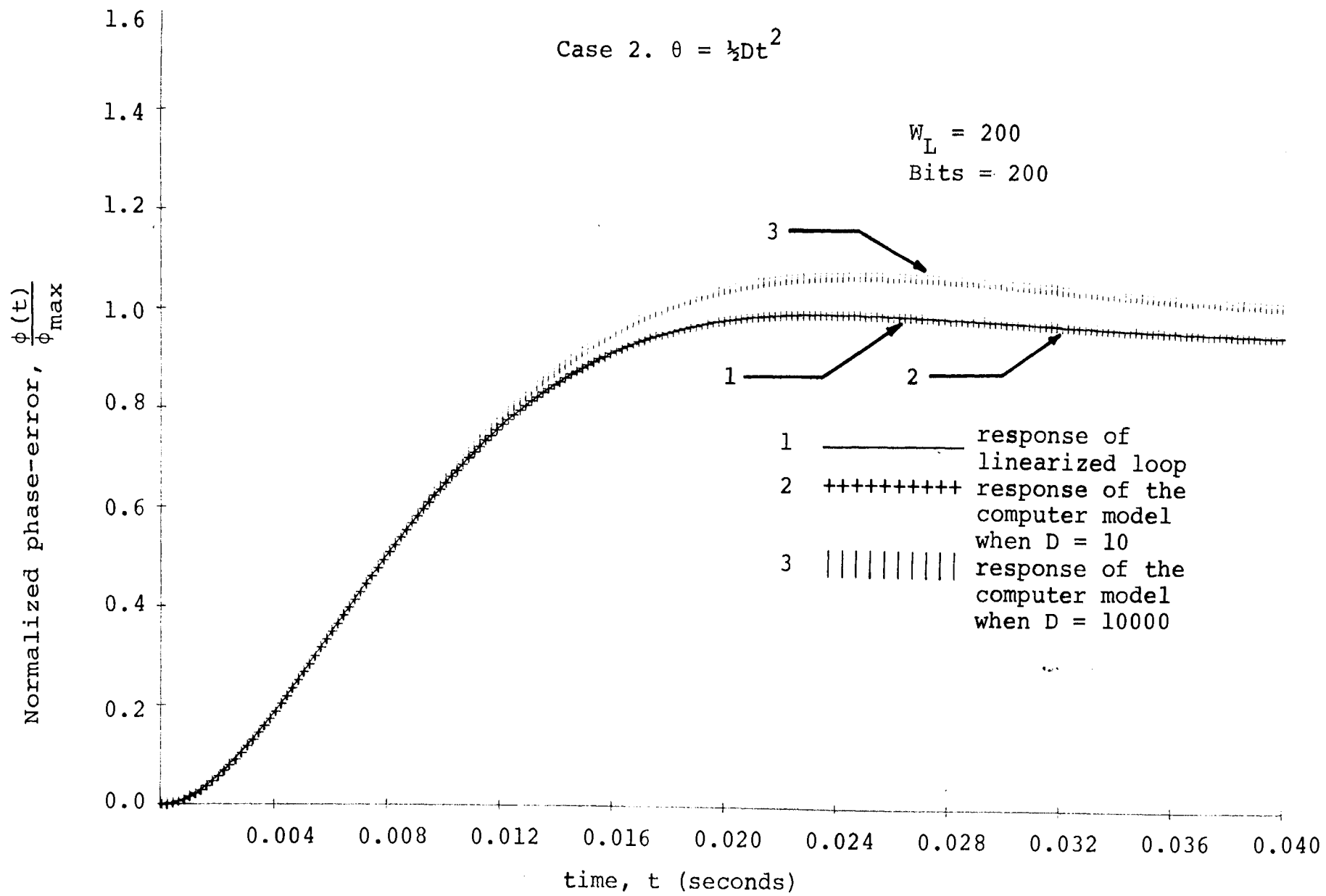


Figure 4. Transient Response of the Model-Noiseless Case 2.

for the random number generators had a significant influence on the number of replications of the simulation model required to reach steady state conditions. Good seeds were selected by trial and error. The sample mean and standard deviation of the output of the Gaussian random number generator used to generate the noise samples were plotted against the number of iterations. The two seeds selected for generating $n_1(t)$ and $n_2(t)$ were the ones that generated processes for which the mean and the standard deviation settled down to their nominal values in minimum number of iterations. Example of the effect of seed selection is given in Fig. 5.

4. Selecting the number of initial bits which could be considered as the transient response of the model

The initial bits that constitute the transient response of the model are omitted from the calculation of bit-error probability, mean-square error, cycle-skips, etc. to allow the transient response of the model to die out. The number of bits omitted was selected in conjunction with step 3 above, and for the parameters and bit-rates chosen was about 200 bits, as can be seen from Fig. 5.

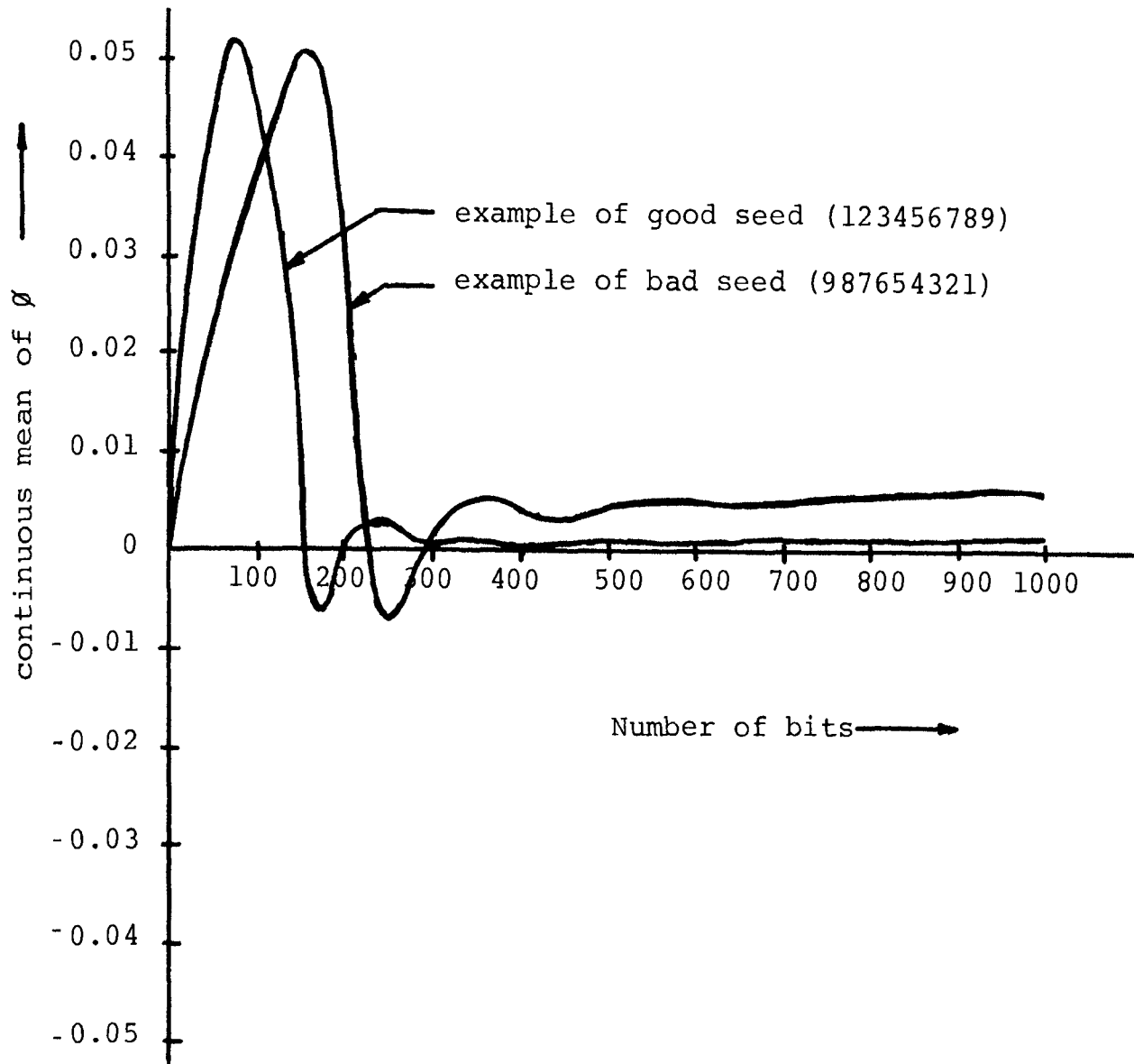


Figure 5: Example of the Effect of Seed Selection

5. Testing the model when Gaussian noise is present

The model was run for signal-to-noise power ratios (noise referred to a bit-rate bandwidth) of 0,1,2,3 and 4 decibels (SNRDB=0,1,2,3 and 4). The bit-error probability P_E obtained from the model was compared with the theoretical values obtained by Didday and Lindsey [5] for a first-order Costas loop (i.e., where LPF3, shown in Figure 1 is absent). This comparison is shown in Table 1.

The phase-error variance is one more yardstick to test the model. The variance σ_{ϕ}^2 of the phase-error was obtained from the model and compared with the theoretical results calculated from a linearized analysis of the loop. It has been shown [5] that for high signal-to-noise power ratios the following approximate relation holds:

$$\sigma_{\phi}^2 = \frac{W_L}{W} \left[\frac{1}{\text{SNRBR}} + \frac{1}{2(\text{SNRBR})^2} \right] \quad (3-9)$$

where SNRBR is the signal-to-Gaussian-noise power ratio in a bit-rate bandwidth. A comparison between σ_{ϕ}^2 obtained from the computer model and the corresponding values for a linearized model given by Eq. (3-9) is presented in Table 2. This was done for SNRDB=7,8, and 9dB.

Table 1: Bit-Error Probability vs SNRDB*

SNRDB	P_E	
	Theoretical	Model + (with limiter)
0	0.078	0.099
1	0.055	0.076
2	0.035	0.041
3	0.022	0.024
4	0.010	0.012

* Signal-to-Gaussian-noise power ratio measured in a bit-rate bandwidth and expressed in decibels.

+ A step-limiter was introduced in the in-phase channel of the Costas loop

Table 2: Phase-Error Variance vs SNRDB

SNRDB	σ_θ^2		
	Theoretical	Model	
		with limiter	without limiter
7	0.00219	0.00295	0.00236
8	0.00171	0.00161	0.00167
9	0.00134	0.00118	0.00120

The mean of the phase-error is expected to be zero because of a zero mean assumed for the Gaussian noise. The values obtained from the computer model were very small, but not quite equal to zero. The reason for this is discussed in the next chapter.

Threshold can be defined as the signal-to-noise ratio at which a loop loses lock which is more or less arbitrarily defined.

An arbitrary method of determining the occurrence of loss of lock in the computer model is used. Each time the absolute value of the phase-error ϕ exceeds the threshold value, $\pi/4$ radian, a cycle-skip results and is noted. A count is also kept of the number of cycle-skips in every ten consecutive input bits, and a loss of lock is said to occur when this count exceeds the value five. The value of the SNR for which this occurs is defined as the threshold value for the model. Also note that after a cycle-skip has been registered, the conditions in the loop (model) are initialized to those at time $t=0$ second.

It has been suggested [5] that threshold occurs in a Costas loop at $\sigma_{\phi}^2 \approx 1/8$. With $W/W_L=100$ in Eq. (3-9), the value used in the model, a threshold of -9.2 dB results (measured in a bit-rate bandwidth).

SPB*	Model (without limiter)	Theoretical	Experimental
10	-10dB ⁺	-9.2dB	-7dB
20	-9dB		

* SPB - Noise samples taken per bit

+ Signal-to-Gaussian-noise power ratio (measured in a bit-rate bandwidth) expressed in decibels.

Table 3: Threshold Results for Costas Loop

Threshold obtained from the model is compared with this value and the previously obtained experimental value, in Table 3.

Results were also obtained for phase-error variance for the case when a limiter was inserted in the in-phase channel of the loop. These results are included in Table 2 and conclusions drawn in the next chapter. The limiting process has an interesting effect on the threshold. This is discussed in the next chapter.

The effect on the threshold of varying the number of samples per input bit was also investigated. The results are included in Table 3 and the comments follow in the next chapter.

B. Results for interference backgrounds

The final step was to obtain results for cw interference once the model was tested and verified (steps 1 through 5).

Bit-error probability and normalized mean-square error between input and output were computed for different signal-to-Gaussian-noise power ratios, interference-to-Gaussian noise power ratios and frequency offsets of the interference. These are compared with previously obtained experimental results in Tables 4 and 5.

SNRDB	INRDB	$\Delta f=10\text{KHz}$		$\Delta f=5\text{KHz}$		$\Delta f=0$	
		Experimental MSE	Model MSE	Experimental MSE	Model MSE	Experimental MSE	Model MSE
7	0	0.140	0.166	0.160	0.168	0.220	0.187
	3	0.140	0.167	0.190	0.171	0.340	0.187
	6	0.155	0.170	0.230	0.175	Lock Lost	0.215
8	0	0.120	0.136	0.130	0.137	0.160	0.150
	3	0.120	0.136	0.150	0.141	0.220	0.162
	6	0.125	0.137	0.170	0.170	Lock Lost	0.179
9	0	0.100	0.108	0.105	0.110	0.140	0.116
	3	0.100	0.108	0.130	0.111	0.175	0.124
	6	0.105	0.109	0.150	0.123	0.330	0.153

Notes: INRDB = cw interference-to-Gaussian-noise power ratio (in decibels)
 Δf = frequency-offset of interference from the carrier frequency f_0 Hz
MSE = normalized mean-square error between input and output

Table 4: Summary of Results for MSE in Presence of cw Interference

SNRDB	INRDB	$\Delta f=10\text{KH}_z$		$\Delta f=5\text{KH}_z$		$\Delta f=0$	
		Experimental P_E	Model P_E	Experimental P_E	Model P_E	Experimental P_E	Model P_E
7	0	0.002	0.001	0.002	0.001	0.010	0.021
	3	0.002	0.001	0.0025	0.001	0.037	0.032
	6	0.002	0.001	0.003	0.002	Lock Lost	0.070
8	0	0.0005	0.001	0.0006	0.001	0.005	0.004
	3	0.0005	0.0	0.0009	0.001	0.015	0.009
	6	0.0005	0.0	0.001	0.002	Lock Lost	0.042
9	0	0.001	0.0	0.0002	0.0	0.002	0.0
	3	0.001	0.0	0.0003	0.0	0.007	0.005
	6	0.0001	0.0	0.0004	0.0	0.030	0.032

Table 5: Summary of Results for P_E in Presence of cw Interference

IV. DISCUSSION OF RESULTS AND CONCLUSIONS

From the results presented in the previous chapter, the following comments can be made and conclusions drawn:

- A. For the ideal noiseless case, the transient response (Figs. 3 and 4) of the model coincided closely with the analytically calculated response of the linearized ($\sin 2\theta \approx 2\theta$) loop, when the conditions of linearity were satisfied. This verified the accuracy of the computer model for noiseless conditions.
- B. Selection of seeds for the random number generators (subroutine GAUSS in the computer program shown in Appendix D) had a significant influence on the length of the initial transient response of the model and on the values for P_E and σ_θ^2 calculated from the model. A bad seed had the effect of increasing the P_E and σ_θ^2 beyond the values expected theoretically, while a good seed tended to produce more acceptable values for these quantities.
- C. For the Gaussian noise case, the P_E calculated from the model was always higher than the theoretically calculated values (Table 1). This can be attributed

to (i) the theoretical values used for comparison are for a first-order Costas loop (i.e. when LPF 3 shown in Figure 1 is absent) while the model is for the second-order Costas loop, and (ii) for the number of noise samples used in the model, the noise may not have been perfectly Gaussian in character. Also, the two noise processes $n_1(t)$ and $n_2(t)$ were not truly independent statistically, as they should be.

- D. For high signal-to-Gaussian-noise ratios (SNRDB= 7,8, and 9), the introduction of a limiter in the in-phase channel of the loop (model) did not have any noticeable effect on the values of σ_ϕ^2 (Table 2). With or without a limiter, the values of σ_ϕ^2 calculated from the model, compared favorably with the theoretical values calculated from Eq. (3-9) which holds for high signal-to-noise ratios.
- E. Without a limiter in the in-phase channel, the value obtained for the threshold was close to the theoretically predicted value in the presence of Gaussian noise alone. Increasing the number of noise samples per bit had the interesting effect of raising the threshold. However, the most

interesting result found was that the limiter in the in-phase channel of the loop had the effect of stabilizing the loop near threshold and as a result, the loop did not go out of lock even at -11dB (SNRDB) and had only 4 cycle-skips in 800 bits.

- F. The results obtained for the cw interference were compared only with previously obtained experimental results. No theoretical results are available in the literature for the performance of Costas loops operating in cw interference. From the majority of the results obtained for the MSE (Table 4) it can be concluded that the effects of interference as obtained with the model were much less severe than shown by the corresponding experimental results. Possible explanations for this are: (i) measurement error in obtaining the experimental results; (ii) inadequate representation of the cw interference in the model. However, no such conclusion could be made from the results for the P_E . For the very low values of P_E corresponding to high SNRDB's, the model did not employ a sufficient number of bits for good accuracy. Only 1000 bits were used due to limited availability of computer time.

REFERENCES

1. Conte, S.D., Elementary Numerical Analysis (1965), McGraw-Hill.
2. Sanneman, R.W., and Rowbotham, J.R., "Unlock Characteristics of the Optimum Type II Phase-Locked Loop", IRE Trans. on Aerospace and Navigational Electronics, Vol. ANE-11 (March 1964), 15-24.
3. Rowbotham, J.R., and Sanneman, R.W., "Random Characteristics of the Type II Phase-Locked Loop", IEEE Trans. on Aerospace and Electronic Systems, Vol. AES-3 (July 1967), 604-612.
4. Smith, A.E., and Johnson, R.S., "A Digital Simulation of a Carrier Demodulation/Tracking Phase-Locked Loop in a Noisy, Multipath Environment", EASCON '68 Record (1968), 206-216.
5. Didday, Richard L. and Lindsey, William C., "Subcarrier Tracking Methods and Communication System Design", IEEE Trans. on Communication Technology, Vol. COM-16 (August 1968), 541-550.

6. Ziemer, R.E., "Experimental Comparison of Costas and PLL Demodulator in RFI Environments", NASA Report (Listed in STAR) No. X-520-69-355 (September 1969).
7. Downing, John J., Modulation Systems and Noise (1964), Englewood Cliffs: Prentice-Hall.
8. Jaffe, R.M., and Rechtin, E., "Design and Performance of Phase-Lock Circuits Capable of Near-Optimum Performance Over a Wide Range of Input Signals and Noise Levels", IRE Trans. on Information Theory, Vol. IT-1 (March 1955), 66-76.
9. Golomb, S.W., Digital Communications with Space Applications (1964), Englewood Cliffs: Prentice-Hall.
10. Carlson, Bruce A., Communication Systems (1968), McGraw-Hill.
11. Nichols, Myron H. and Rauch, Lawrence L., "Telemetry", Prepared for USAF Systems Command Under Contract No. AF 19(628)-4048, ESD-TR-66-464 (July 1966), Chapter 6 (pp. 6.42 to 6.51).

VITA

The author, Ajay Mugatlal Mehta, was born on January 16, 1947 in India. He got his Bachelor's degree in Electrical Engineering with honors at the Indian Institute of Technology, Bombay, in 1968.

He has been enrolled as a Master's candidate in the Electrical Engineering department of the University of Missouri - Rolla since September, 1968.

Mr. Mehta is a member of IEEE and Eta Kappa Nu.

APPENDIX A

FLOW DIAGRAM - NOISELESS CASE

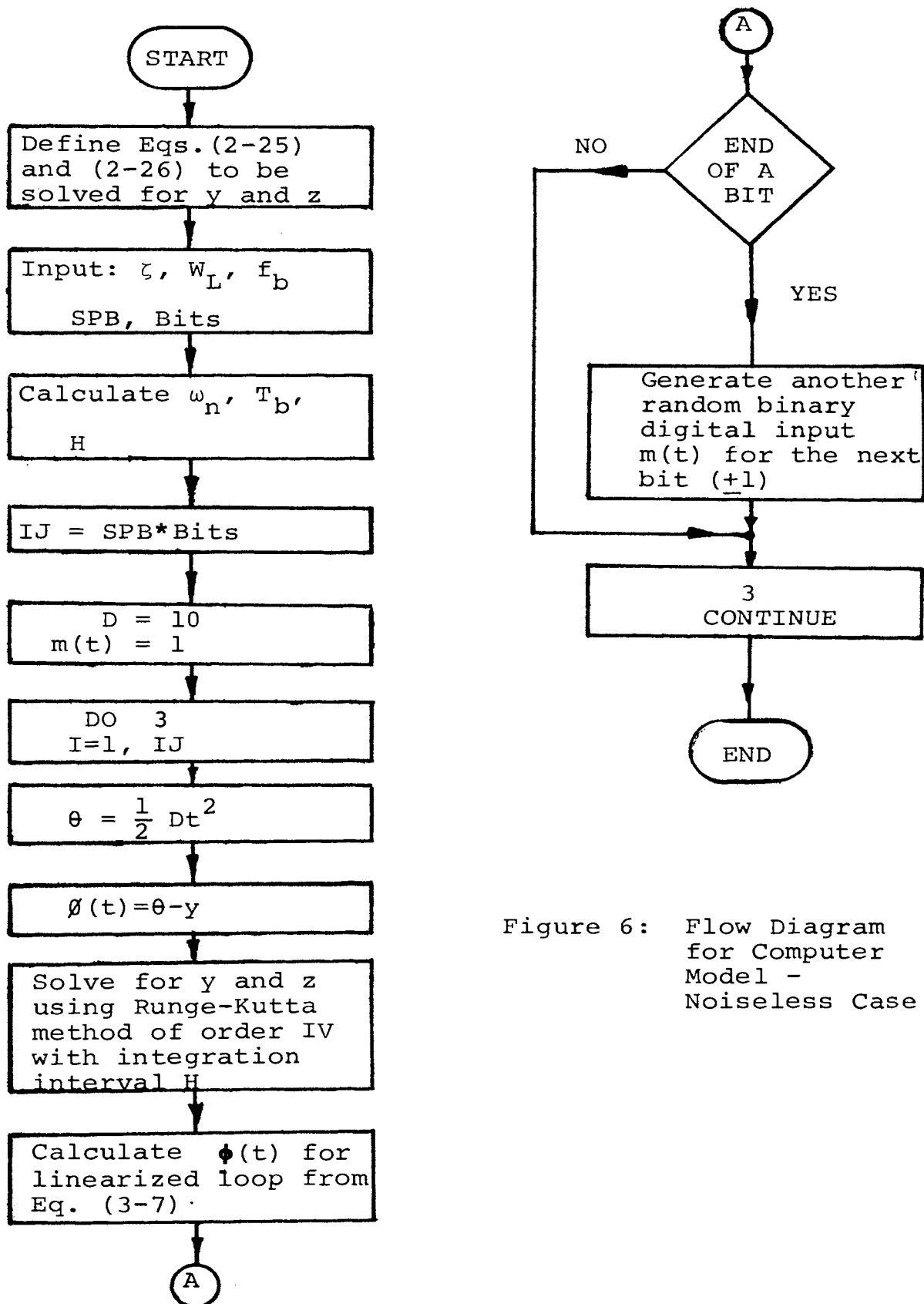


Figure 6: Flow Diagram for Computer Model - Noiseless Case 2

APPENDIX B

COMPUTER PROGRAM - NOISELESS CASE

```

C
C-----
C   COMPUTER PROGRAM FOR DIGITAL SIMULATION OF COSTAS LOOP OPERATION
C-----
C   CASE OF LINEARLY INCREASING FREQUENCY AT THE INPUT
C-----
C   P1 STORES THE VALUE OF PHI AT THE END OF EACH BIT, TPHI STORES THE
0001  C   THEORETICALLY CALCULATED VALUE OF PHI AT THE END OF EACH BIT
C   DIMENSION P1(200),TPHI(200)
C-----
C   DEFINE THE TWO SIMULTANEOUS DIFFERENTIAL EQUATIONS OF THE COSTAS LOOP
C   T - TIME IN SECONDS, Y = ̸ , Z - DUMMY VARIABLE INTRODUCED
0002  C   F1(T,Y,Z)=Z+2.*ZETA*WN*V5
0003  C   G1(T,Y,Z)=WN*WN*V5
C-----
C   ZETA - DAMPING FACTOR, WL - EQUIVALENT NOISE BANDWIDTH
C   WN - NATURAL FREQUENCY, WI - INPUT SIGNAL BANDWIDTH
C   FB - BIT-RATE BANDWIDTH, TB - PERIOD OF AN INPUT BIT
C   SPB - GAUSSIAN-NOISE SAMPLES TAKEN PER BIT, BITS -
C   TOTAL NUMBER OF BITS CONSIDERED, H - INTEGRATION AND
C   SAMPLING INTERVAL, SAMPLE - TOTAL NUMBER OF SAMPLES
C   F - MODULATING DIGITAL SIGNAL
C-----
0004  ZETA=0.707
0005  PI=3.1416
0006  WL=200.
0007  WN=4.*ZETA*WL/(1.+4.*ZETA**2)
0008  WI=10000.
0009  FB=WI/2.
0010  TB=1./FB
0011  SPB=20.
0012  NSPB=SPB
0013  BITS=200.
0014  NMAX=BITS
0015  H=TB/SPB
0016  SAMPLE=SPB*BITS
0017  IJ=SAMPLE
0018  CALL PENPGS(12HMEHTA AJAY M,12,1)

```



```

C
C
0019      D - RATE OF INCREASE IN THE INPUT FREQUENCY (HZ/SEC)
          D=10.
C
C
0020      DO LOOP FOR TWO VALUES OF D (D = 10, CONDITION OF LINEARITY
          SATISFIED ; AND D = 10000, NONLINEAR CASE)
          DO 55 K=1,2
C
0021      T=0.
0022      Y=0.
0023      Z=0.
0024      F=1.
0025      T*PHI(1)=0.
0026      P1(1)=0.
C
C
0027      MAIN DO LOOP PERFORMING ITERATIONS
          DO 3 I=1,IJ
C
0028      THETA=D*T*T/2.
0029      PHI=THETA-Y
0030      V3=F*COS(PHI)
0031      V4=F*SIN(PHI)
0032      V5=V3*V4
C
C
          EMPLOYING RUNGE-KUTTA METHOD OF ORDER IV TO SOLVE THE LOOP EQUATIONS
C
0033      A1=H*F1(T,Y,Z)
0034      B1=H*G1(T,Y,Z)
0035      A2=H*F1(T+H/2.,Y+A1/2.,Z+B1/2.)
0036      B2=H*G1(T+H/2.,Y+A1/2.,Z+B1/2.)
0037      A3=H*F1(T+H/2.,Y+A2/2.,Z+B2/2.)
0038      B3=H*G1(T+H/2.,Y+A2/2.,Z+B2/2.)
0039      A4=H*F1(T+H,Y+A3,Z+B3)
0040      B4=H*G1(T+H,Y+A3,Z+B3)
0041      Y=Y+(A1+2.*A2+2.*A3+A4)/6.
0042      Z=Z+(B1+2.*B2+2.*B3+B4)/6.
0043      T=T+H
C

```

```

0044      C      CHECK FOR THE END OF A BIT
           IF(MOD(I,NSPB))3,4,3
0045      C      4 CONTINUE
0046      J=I/SPB+1.
0047      PI(J)=PHI
0048      TPHI(J)=D*(1.-1.414*EXP(-WN*T*0.707)*COS(WN*T*0.707-PI/4.))/WN/WN
           C
           C      GENERATING A RANDOM DIGITAL MODULATING SIGNAL
           C
0049      ZZ=RAND(0)
0050      IF(ZZ.LT.0.5)F=-1.
0051      IF(ZZ.GE.0.5)F=1.
           C
0052      3 CONTINUE
0053      PHIMIN=0.
0054      PHIMAX=D*(1.+EXP(-PI))/WN/WN
0055      WRITE(3,100)PHIMIN,PHIMAX
0056      100 FORMAT(1H,'PHIMIN =',F7.4,10X,'PHIMAX =',F7.4)
0057      YMIN=1.6*PHIMIN
0058      YMAX=1.6*PHIMAX
0059      CALL NEWPLT(2.0,2.0,10.0)
0060      CALL ORIGIN(0.0,0.0)
0061      CALL TSCALE(0.0,BITS*TB,8.0)
0062      CALL YSCALE(YMIN,YMAX,5.0)
0063      CALL TPLT(PI,NMAX,2,10*(K-1)+3)
0064      D=10000.
0065      55 CONTINUE
0066      CALL NEWPLT(2.0,2.0,10.0)
0067      CALL ORIGIN(0.0,0.0)
0068      CALL TSCALE(0.0,BITS*TB,8.0)
0069      CALL YSCALE(YMIN,YMAX,5.0)
0070      CALL TPLT(TPHI,NMAX,1,-1)
0071      CALL TAXIS(SPB*TB)
0072      CALL YAXIS(PHIMAX/5.)
0073      CALL ENDPLT
0074      CALL LSTPLT
0075      CALL EXIT
0076      STOP
0077      END

```

APPENDIX C

FLOW DIAGRAM - GAUSSIAN NOISE AND
CW INTERFERENCE PRESENT

Nomenclature for notations used in Appendix C
(but not defined earlier)

Bits - Total number of bits considered

OMIT - Number of initial bits omitted as
transient response of the computer
model

IJ - Total number of noise samples
considered

NI - Number of initial samples omitted
as transient response

NUSKIP-Count of the number of cycle-skips
per every 10 consecutive bits

NSKIP- Number of cycle-skips

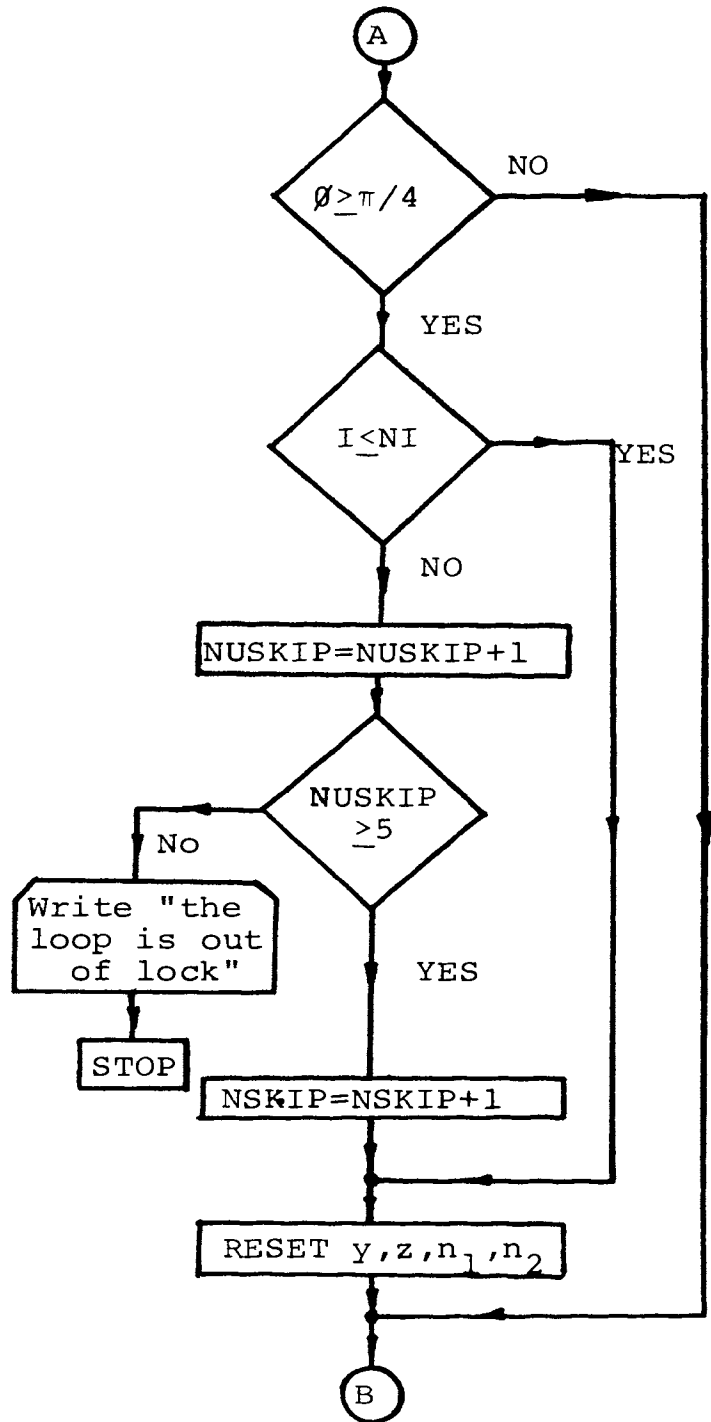
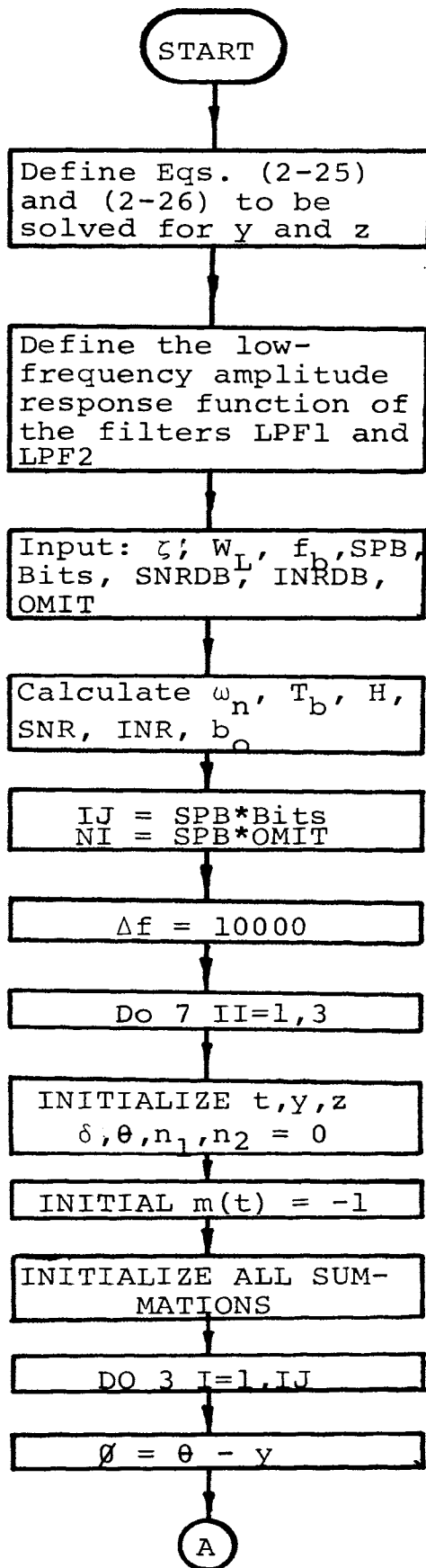


Figure 7: Flow Diagram for Computer Model - Gaussian Noise Plus cw Interference Present

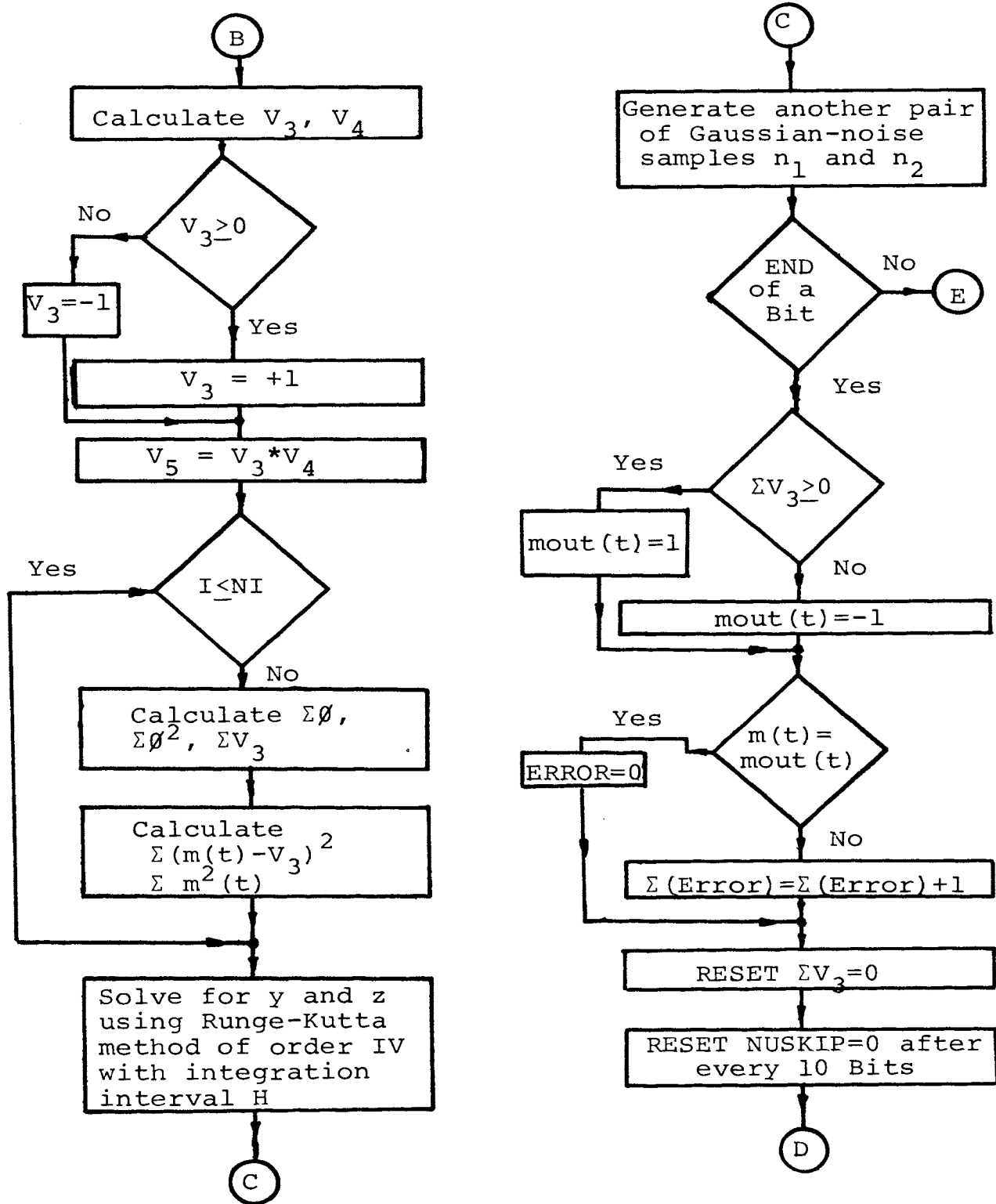


Figure 7 (contd.): Flow Diagram for Computer Model - Gaussian Noise Plus cw Interference Present

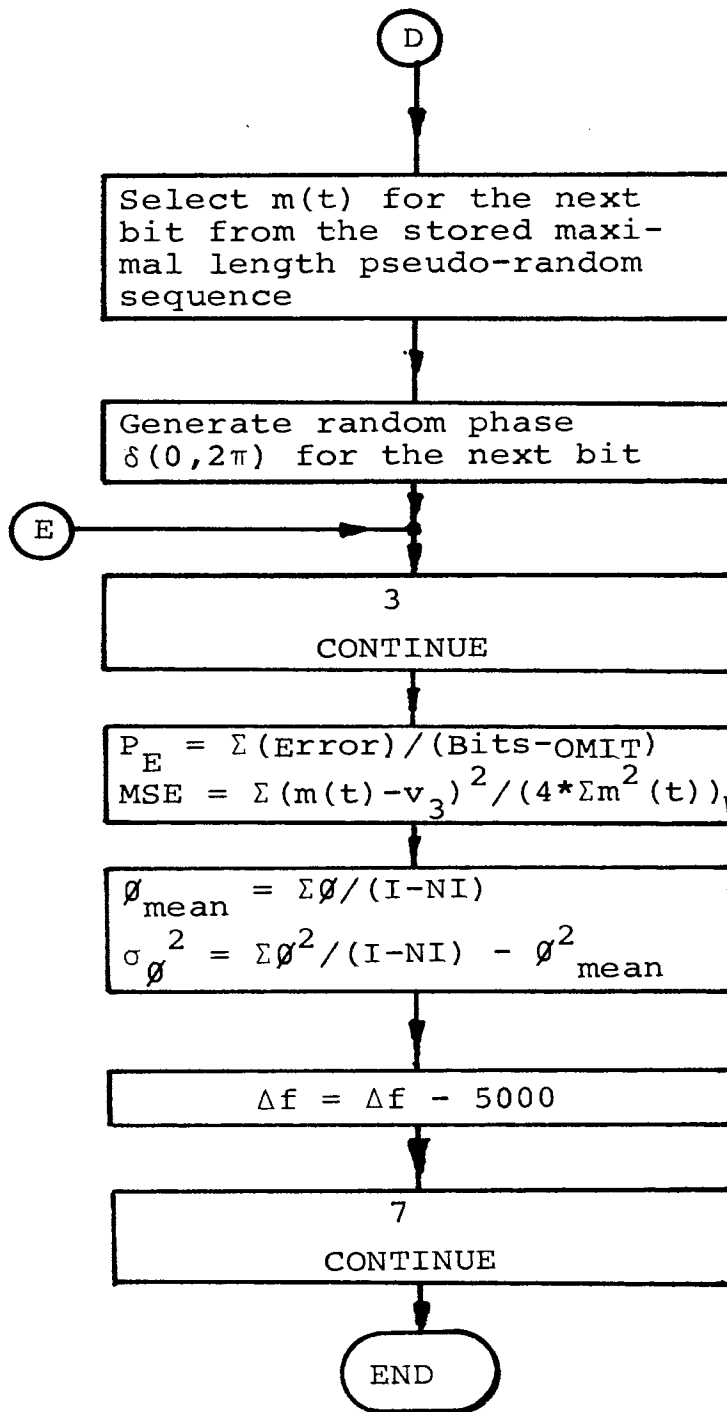


Figure 7 (contd.): Flow Diagram for Computer Model - Gaussian Noise Plus cw Interference

APPENDIX D

COMPUTER PROGRAM - GAUSSIAN NOISE
AND CW INTERFERENCE PRESENT

```

C
C   COMPUTER PROGRAM FOR DIGITAL SIMULATION OF COSTAS LOOP OPERATION
C   -----
C   CASE OF SIGNAL CORRUPTED BY GAUSSIAN NOISE AND CW INTERFERENCE
C
0001 REAL*4 INR,INROB,N1,N2
0002 DIMENSION F2(31)
0003 DIMENSION IJKLM(3),JKLMN(3)
C
C   DEFINE THE TWO SIMULTANEOUS DIFFERENTIAL EQUATIONS OF FIRST-ORDER
C   DESCRIBING THE COSTAS LOOP
C   T - TIME IN SECONDS, Y -  $\theta$ , Z - DUMMY VARIABLE INTRODUCED
0004 E1(T,Y,Z)=Z+2.*ZETA*WN*V5
0005 G1(T,Y,Z)=WN*WN*V5
C
C   DEFINE AMPLITUDE RESPONSE FUNCTION OF THE FILTERS LPF 1 AND LPF 2
C   FOR THE LOW-FREQUENCY COMPONENTS OF THE CW INTERFERENCE
0006 RB(DELTA,F,N,ALPHA)=1./(1.+(DELTA/F/ALPHA)**N)
0007 N=2
0008 ALPHA=5.3E3
C
C   CONSTANTS AND PARAMETERS DEFINED
0009 PI=3.1416
0010 THRESH=PI/4.
C
C   ZETA - DAMPING FACTOR, WL - EQUIVALENT NOISE BANDWIDTH
C   WN - NATURAL FREQUENCY, WI - INPUT SIGNAL BANDWIDTH
C   FB - BIT-RATE BANDWIDTH, TB - PERIOD OF AN INPUT BIT
C   SPB - GAUSSIAN-NOISE SAMPLES TAKEN PER BIT, BITS -
C   TOTAL NUMBER OF BITS CONSIDERED, H - INTEGRATION AND
C   SAMPLING INTERVAL, SAMPLE - TOTAL NUMBER OF SAMPLES
C   F - MODULATING DIGITAL SIGNAL, CMIT - NUMBER OF INITIAL
C   BITS OMITTED AS TRANSIENT RESPONSE OF THE MODEL
C
0011 ZETA=0.707
0012 WL=100.
0013 WN=4.*ZETA*WL/(1.+4.*ZETA**2)
0014 WI=10000.
0015 FB=WI/2.
0016 TB=1./FB
0017 SPB=20.

```



```

0018      NSPB=SPB
0019      OMIT=200.
0020      NI=OMIT*SPB
0021      H=TB/SPB
0022      BITS=700.
0023      SAMPLE=SPB*BITS
0024      IJ=SAMPLE

C
C
0025      DEFINE THE MAXIMAL-LENGTH PSEUDO-RANDOM DIGITAL MODULATING
C      SEQUENCE OF +1'S AND -1'S
C      READ(1,201)(F2(L), L=1,31)

C
C      INPUT : SIGNAL-TO-GAUSSIAN-NOISE POWER RATIO IN DECIBELS
0026      READ(1,104)SNRDB
0027      SNR=10.**(SNRDB/10.)

C
C      CALCULATE THE STANDARD DEVIATION OF RANDOM GAUSSIAN SAMPLING
C      PROCESSES N1 AND N2
0028      STDDEV=SQRT(SPB/SNR/2.)

C
C      CALCULATE ESTIMATED VALUE OF VARIANCE(PHI), HOLDS GOOD AT HIGH SNR'S
0029      VARPHI=WL/WI*(1./SNR+0.5/SNR**2)

C
C      INPUT : INTERFERENCE-TO-GAUSSIAN-NOISE POWER RATIO IN DECIBELS
0030      READ(1,104)INRDB
0031      INR=10.**(INRDB/10.)

C
C      CALCULATE THE AMPLITUDE OF CW INTERFERENCE
0032      B=SQRT(INR/SNR)

C
C      DO LOOP FOR DIFFERENT VALUES OF FREQUENCY-OFFSET OF INTERFERENCE
C
0033      DELTAF=10000.
0034      DO 7 II=1,3
0035      WRITE(3,101)SNRDB,STDDEV,INRDB,N,ALPHA,DELTAF
0036      JKLMN(II)=123456789
0037      IJKLM(II)=753214587
0038      C=BR(DELTAF,N,ALPHA)
0039      DELTAW=2.*PI*DELTAF

C
C      INITIALIZE THE CONDITION OF THE LOOP
C

```

```

0040      T=0.
0041      Y=0.
0042      Z=0.
0043      F=-1.
-----
0044      N1=0.
0045      N2=0.
0046      RIGPHI=0.
0047      RIGPH2=0
0048      RIGERR=0.
0049      RIGQ=0.
0050      RIGF2=0.
0051      RIGFQ2=0.
0052      DELTA=0.
0053      THETA=0.
0054      NUSKIP=0
0055      NSKIP=0
-----
0056      C      MAIN LOOP PERFORMING ITERATIONS
          C      DO 3 I=1,IJ
-----
0057      C      PHI = PHASE ERROR
          C      PHI=THETA-Y
-----
0058      C      CHECK FOR A CYCLE-SKIP
          C      IF (ABS(PHI).GE.THRESH)GO TO 11
-----
0059      C      GO TO 12
0060      11     CONTINUE
0061      C      IF (I.LE.NT)GO TO 20
0062      C      NUSKIP=NUSKIP+1
-----
0063      C      IF NUMBER OF CYCLE-SKIPS PER EVERY 10 CONSECUTIVE BITS IS GREATER
          C      THAN 5, DECLARE THE LOOP AS BEING OUT OF LOCK
0064      C      IF (NUSKIP.GE.5)GO TO 66
0065      20     CONTINUE
          C      NSKIP=NSKIP+1
-----
0066      C      IN CASE OF CYCLE-SKIP, RESET THE CONDITION OF THE LOOP AS AT TIME
          C      T=0, THIS IS EQUIVALENT TO MANUALLY RESETTING IN AN EXPERIMENT
0067      C      PHI=0.
0068      C      Y=0.
0069      C      Z=0.
0070      C      N1=0.
          C      N2=0.
-----
0071      C      GO TO 12

```

```

0072      66 WRITE(3,103)
0073      STOP
0074      12 CONTINUE
0075      X=DELTA*W*DELTA
0076      V3=(F+N2+B*C*COS(X))*COS(PHI)-(N1+B*C*SIN(X))*SIN(PHI)
0077      V4=(F+N2+B*C*COS(X))*SIN(PHI)+(N1+B*C*SIN(X))*COS(PHI)
      C
      C CASE OF OUTPUT THROUGH A LIMITER IN THE IN-PHASE CHANNEL OF THE LOOP
0078      IF(V3.GE.0.)V3=1.
0079      IF(V3.LT.0.)V3=-1.
      C
0080      V5=V3*V4
0081      IF(I.LE.N1)GO TO 21
0082      BIGPHI=BIGPHI+PHI
0083      BIGPH2=BIGPH2+PHI*PHI
0084      Q=V3
0085      FQ=F-Q
0086      BIGQ=BIGQ+Q
0087      BIGFQ2=BIGFQ2+FQ*FQ
0088      BIGF2=BIGF2+(F-(-F))**2
0089      21 CONTINUE
      C
      C RUNGE-KUTTA METHOD OF ORDER IV USED FOR NUMERICAL INTEGRATION
      C
0090      A1=H*F1(T,Y,Z)
0091      B1=H*G1(T,Y,Z)
0092      A2=H*F1(T+H/2.,Y+A1/2.,Z+B1/2.)
0093      B2=H*G1(T+H/2.,Y+A1/2.,Z+B1/2.)
0094      A3=H*F1(T+H/2.,Y+A2/2.,Z+B2/2.)
0095      B3=H*G1(T+H/2.,Y+A2/2.,Z+B2/2.)
0096      A4=H*F1(T+H,Y+A3,Z+B3)
0097      B4=H*G1(T+H,Y+A3,Z+B3)
0098      Y=Y+(A1+2.*A2+2.*A3+A4)/6.
0099      Z=Z+(B1+2.*B2+2.*B3+B4)/6.
0100      T=T+H
      C
      C GENERATE SAMPLES FOR THE TWO RANDOM GAUSSIAN PROCESSES N1 AND N2
0101      CALL GAUSS(IJKLMN(I1),STDDEV,0.,N1)
0102      CALL GAUSS(JKLMN(J1),STDDEV,0.,N2)
      C
      C CHECK FOR THE END OF A BIT
0103      IF(MOD(I,NSPB))3,4,3
      C
0104      4 CONTINUE

```

```

0105      J=FLOAT(I)/SPB
0106      IF(J.LE.200)GO TO 22
0107      IF(MOD(J,10).EQ.0)NUSKIP=0
0108      IF(BIGQ.LT.0.)FOUT=-1.
0109      IF(BIGQ.GE.0.)FOUT=1.
      C
0110      C      COMPUTING THE NUMBER OF ERRORS
      C      IF(F.NE.FOUT)BIGERR=BIGERR+1.
      C
0111      BIGQ=0.
0112      22  CONTINUE
0113      JJ=MOD(J+1,31)
0114      IF(JJ.EQ.0)JJ=31
      C
0115      C      GENERATING A PSEUDO-RANDOM FINITE-LENGTH DIGITAL MODULATING SIGNAL
      C      F=F2(JJ)
      C
      C      GENERATING A RANDOM PHASE, DELTA, FOR THE CW INTERFERENCE
0116      ZZ=RAND(0)
0117      DELTA=2.*PI*ZZ
      C
0118      3  CONTINUE
      C
      C      PE - BIT-ERROR PROBABILITY, SOMEAN - MEAN-SQUARE
      C      ERROR BETWEEN INPUT AND OUTPUT, PHIM - MEAN OF PHI
      C      PHIVAR - VARIANCE OF PHI
      C
0119      PE=BIGERR/(BITS-OMIT)
0120      SOMEAN=BIGFQ2/BIGF2
0121      PHIM=BIGPHI/(BITS-OMIT)
0122      PHIVAR=BIGPH2/(BITS-OMIT)-PHIM**2
0123      WRITE(3,100)PE,SOMEAN,PHIM,PHIVAR,NSKIP
0124      WRITE(3,100)PE,SOMEAN,PHIM,VARPHI,NSKIP
0125      DELTAF=DELTAF-5000.
0126      7  CONTINUE
0127      100  FORMAT(/1X,'PE='F5.3,10X,'MEAN SQ. ERR.='F9.4,10X,'MEAN PHI='F8.
/5,10X,'VAR. PHI='F12.5,10X,'CYCLES SKIPPED='I3)
0128      101  FORMAT('1','SNRDB = ',F5.1,10X,'STD. DEVIATION = ',F7.4,10X,'INRDB
/='F5.1/' N = ',I1,10X,'ALPHA = ',E16.7,10X,' DELTAF = ',E16.7)
0129      103  FORMAT(/10X,'THE LOOP IS OUT OF LOCK'//)
0130      104  FORMAT(F7.2)
0131      201  FORMAT(F4.1)
0132      STOP
0133      END

```